Journal of Sustainability Science and Management
Volume 17 Number 4, April 2022: 32-48
eISSN: 2672-7226

MICROWAVE-ASSISTED SYNTHESIS, CHARACTERIZATION AND ANTICANCER ACTIVITY OF TETRANUCLEAR SCHIFF BASE COMPLEXES

SITI SOLIHAH KHAIDIR[1]*, HADARIAH BAHRON[1,2], AMALINA MOHD TAJUDDIN[1,3] AND KALAVATHY RAMASAMY[4,5]

[1]Faculty of Applied Sciences, Universiti Teknologi MARA, 40450 Shah Alam, Selangor, Malaysia. [2]University Malaya Centre for Ionic Liquid (UMCIL), Department of Chemistry, Faculty of Science, Universiti Malaya, Kuala Lumpur 50603, Malaysia. [3]Atta-ur-Rahman Institute for Natural Product Discovery (AuRIns), Universiti Teknologi MARA, Selangor, Malaysia. [4]Faculty of Pharmacy, Universiti Teknologi MARA, 42300 Bandar Puncak Alam, Selangor, Malaysia. [5]Collaborative Drug Discovery Research (CDDR) Group, Pharmaceutical and Life Sciences Community of Research, Universiti Teknologi MARA, 40450 Shah Alam, Selangor, Malaysia.

**Corresponding author: s.solihah92@gmail.com*
Submitted final draft: 17 October 2021 *Accepted: 13 November 2021* http://doi.org/10.46754/jssm.2022.4.003

Abstract: A hexadentate Schiff base 6,6'-((*1E,1'E*)-(1,3-phenylenebis(azanylylidene)) bis(methanylylidene))bis-(2-methoxyphenol) (L) was synthesized via condensation of *o*-vanillin and *m*-phenylenediamine. Its tetranuclear Cu(II), Co(II) and Zn(II) complexes were obtained through microwave-assisted complexation with corresponding acetate salts in a 1:2 ratio of L:M. The compounds were elucidated through CHN elemental analysis, molar conductivity, magnetic susceptibility (MSB), thermogravimetric analysis (TGA), Infrared (IR), UV-Visible, ^{1}H and ^{13}C NMR spectroscopy. The ν(C=N), $\nu(C\text{-}O)_{phenolic}$ and $\nu(C\text{-}O)_{methoxy}$ peaks shifted to higher wavenumber upon complexation, with the appearance of new peaks assignable to ν(M-N) and ν(M-O) at 651-671 and 424-441 cm^{-1}, respectively, indicating that L coordinated to metal centres through its azomethine N, phenolic O and methoxy O. The $Cu_4(L)_2$ and $Co_4(L)_2$ complexes were paramagnetic with μ_{eff} of 1.85 and 3.84 B.M., respectively; whereas the $Zn_4(L)_2$ displayed the expected diamagnetism. The thermal decomposition of all complexes showed a two-stage process at around 100°C and 300°C. An anticancer investigation against human colorectal cancer (HCT116) cell lines revealed that the parent ligand possessed lower activity than its metal complexes. $Cu_4(L)_2$ exhibited the highest anticancer activity with IC_{50} of 6.56 ± 1.26 μM.

Keywords: Microwave-assisted synthesis, tetranuclear complexes, Schiff base, anticancer.

Introduction

Schiff bases are widely used as ligands due to their ability to stabilize metals in various oxidation states (Al-Shaalan, 2011; Bader, 2010). Schiff bases with chelating ability are in demand because of their facile preparation (Bahron *et al.,* 2007; Malinkin *et al.,* 2012) from easily available and relatively inexpensive starting materials. Schiff bases are products of the condensation reaction of primary amines with active carbonyl compounds (Mesbah *et al.,* 2018; Ghani *et al.,* 2014). The structure contains imine moiety with general formula of RR'C=N-R" where R is an aryl group, R' is hydrogen and R" are alkyl or aryl group.

Since the introduction of imines in 1864 by Hugo Schiff, hence the name Schiff bases, chemists have carried out extensive research on this family of compounds. In the last few decades, attempts to carry out green practices in synthesis have increased exponentially, where the formation of Schiff bases and their complexes are not excluded (Mane *et al.,* 2011; Tanaka & Toda, 2000; Saikia *et al.,* 2011; Saini *et al.,* 2014). Microwave assisted synthesis is one of the components of green chemistry that has become increasingly popular among coordination chemists particularly for the formation of high nuclearity complexes that conventionally involves long refluxing hours (Kassim & Hamali, 2017; Bahron *et al.,* 2017). Microwave synthesis that involves microwave irradiation (Chakraborty *et al.,* 2012) as a non-conventional energy source (Mermer *et al.,* 2019) appeals to many chemists mainly because of their elegance, high percentage yield, short

reaction period and eco-friendly conditions (Mohanan *et al.,* 2008; Mishra *et al.,* 2016).

The metal complexes of Schiff bases have been reported to exhibit bioactivities such as antibacterial (El-Wahab *et al.,* 2004; Nithya *et al.,* 2018), antiviral (Chang *et al.,* 2010) and antitumor properties (Ebrahimipour *et al.,* 2015; Shabbir *et al.,* 2017; Ahamad *et al.,* 2019). Certain Schiff bases and their complexes display interesting biological properties because their structures allow them to interact beneficially with biological systems (Dave *et al.,* 2014) for example, the ability to interact with DNA (Ray *et al.,* 2009) of cancerous cells that could inhibit cell proliferation. There has been significant interest in complexes that can bind or cleave DNA molecules at specific sites (Dede *et al.,* 2009) because they may play significant role in the genomic investigation and in photodynamic therapy against cancer (Bahron *et al.,* 2019). Mononuclear Schiff base complexes have been commonly reported to be bioactive, but similar reports on tetranuclear complexes derived from phenylenediamine are scarce.

The present work describes the conventional synthesis of Schiff bases, microwave-assisted syntheses of its tetranuclear copper(II), cobalt(II) and zinc(II) complexes, structure elucidation through spectral and physicochemical means and anticancer screening against colon cancer cell lines (HCT116).

Materials and Methods

Materials

O-vanillin (OVan), *m*-phenylenediamine (MPD), cobalt(II) acetate tetrahydrate, copper(II) acetate monohydrate, zinc(II) acetate dihydrate, triethylamine (TEA), absolute ethanol and acetonitrile (ACN) were purchased from Sigma Aldrich (St Louis, US). All chemicals and solvents were analytical grade and were used as received without further purification.

Synthesis of Ligand (L)

The synthesis of the ligand L is represented in Scheme 1. OVan (4.5645 g, 30 mmol) and MPD (1.6221 g, 15 mmol) were dissolved in absolute ethanol (20 mL) and was subjected to reflux for 1 hour. Upon cooling, an orange crystalline solid was formed. It was filtered off and washed with cold methanol before being dried in the air and kept in a desiccator. Recrystallization was carried out through the layering technique where a DMF solution of L was layered with absolute ethanol in a 1:1 volumetric ratio and left undisturbed overnight to produce orange-colored single crystals.

Elemental analysis for L, analysed as $C_{22}H_{20}N_2O_4$: Found (Calc.) C 70.18 (70.12) H 5.36 (5.15) N 7.14 (7.44) %. IR bands (KBr pellet, cm^{-1}): 1617, 1273, 1251. ^{1}H NMR (500 MHz, $CDCl_3$): δ 13.15 (s, 1H), 9.05 (s, 1H), 7.56 (m,1H), 7.55 (mm, 1H), 7.39 (dd, J= 8.0, 1.4 Hz, 1H), 7.16 (dd, J= 7.90 Hz, 1H), 6.94 (t, J= 8.0, 1.4 Hz, 1H), 3.37 (s, 3H).^{13}C NMR δ (ppm): 163.44 (C-OH), 151.45 (C=N), 149.52-113.73 (Ar-C), 56.25 (-OCH_3).

Synthesis of Tetranuclear Complexes $M_4(L)_2$

The tetranuclear complexes, namely $Cu_4(L)_2$, $Co_4(L)_2$ and $Zn_4(L)_2$ were synthesized as shown in Scheme 2. The ligand L (0.8 mmol, 0.3011 g) and appropriate metal acetate salts (1.6 mmol)

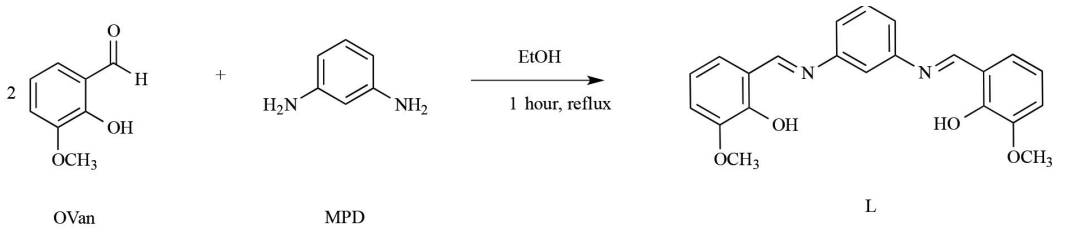

OVan MPD L

Scheme 1: Synthesis of ligand (L)

were mixed in a 2:1 mixture of absolute ethanol: chloroform (10 mL). A few drops of TEA were added dropwise into the mixture and the vial was placed in the microwave. The stirrer speed and reaction time were set at 1000 rpm for 10 minutes, respectively. The reaction mixture was left to cool slowly to attain the room temperature and kept overnight in the chiller. The colored precipitate obtained was washed several times with cold ethanol, filtered off and dried in air.

Elemental analysis for $Cu_4(L)_2$ analysed as $C_{44}H_{36}Cu_4N_4O_8(CH_3CO_2)(H_2O)_3$: Found (Calc.) C 49.50 (49.02) H 4.28 (4.06) N 5.34 (5.02) %. IR (cm^{-1}): 1605, 1597, 1245, 1226, 542, 441. μ_{eff} = 1.85 B.M. Colour: Brown.

Elemental analysis for $Co_4(L)_2$, analysed as $C_{44}H_{36}Co_4N_4O_8(H_2O)_3$: Found (Calc.) C 52.11 (52.71) H 4.89 (3.82) N 4.98 (5.59) %. IR (cm^{-1}): 1602, 1242, 1219, 525, 425. μ_{eff} = 3.84 B.M. Colour: Dark brown.

Elemental analysis for $Zn_4(L)_2$ analysed as $C_{44}H_{36}N_4O_8Zn_4$ (H_2O): Found (Calc.) C 51.80 (51.39) H 5.24 (5.72) N 4.35 (5.45) %. IR (cm^{-1}): 1608, 1242, 1200, 529, 424. μ_{eff} = 0 B.M. Colour: Yellow.

Instruments and Physical Measurements

Elemental analysis for (C H N) were performed with a Thermo Finnigan Flash EA 110 Elemental Analyzer. The FT-IR spectra were recorded as KBr discs (4000-400 cm^{-1}) using Perkin-Elmer FT-IR 1600 spectrometer. Molar conductance of the complexes was recorded in ACN with concentration of 10^{-3} M using Mettler Toledo 730 Series conductivity, while magnetic susceptibility measurements were performed on solid compounds using Sherwood Auto balance. Stuart Melting Point SMP10 apparatus was used to measure the melting points and thermal decomposition data were obtained using a TA Instruments Q50 TGA under nitrogen atmosphere at the heating rate of 10°C min^{-1} from room temperature to 723K. The ^1H and ^{13}C NMR spectra were obtained with a Bruker Avance 500 MHz NMR spectrometer in $CDCl_3$ solvent. Chemical shifts (δ) were reported in ppm relative to TMS. Mass spectral data are measured in MeCN (70%) and H_2O (30%) on ESI-LCMS QQQ Agilent 6410. UV-Visible spectra were obtained in ACN (10^{-4} M) on a Perkin Elmer Lambda 25 UV/Vis Spectrometer. Microwave-assisted syntheses were performed in a Monowave 450 reactor.

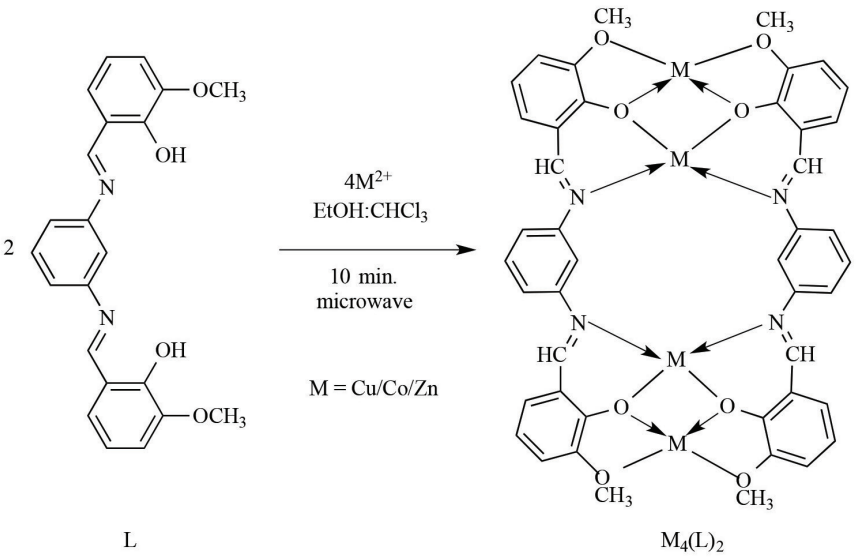

Scheme 2: Synthesis of tetranuclear metal complexes $M_4(L)_2$ where M = Cu, Co and Zn

X-ray Crystallographic Analysis

A suitable single crystal of L ligand was selected and mounted on a glass fiber with epoxy cement. Agilent Technologies SuperNova Dual CCD with an Atlas detector fitted with Mo Kα (λ = 0.71073 Å) radiation at 100 K was used to collect the crystallographic data. Crys Alis PRO (Agilent Technologies, 2014) was used to process the data and performed the absorption corrections. Structure solving and refinement were carried out with SHELX programs (Sheldrick, 2015) integrated into Olex2 (Dolomanov *et al.,* 2009). Full-matrix least-squares refinement F^2 was carried out and all non-hydrogen atoms were refined anisotropically. The C-bound H atoms were placed on stereochemical grounds and refined in the riding model approximation with U_{iso} = 1.2–1.5U_{eq} (carrier atom). SHELXTL and MERCURY software were used to create the molecular graphics for publication. The PLATON program was also used to calculate the molecular structure of the crystal (Sheldrick, 1997).

Anticancer Screening

Cell Culture

The human colorectal carcinoma cell line, HCT116 (ATCC® CCL-247™) was cultured in the Roswell Park Memorial Institute RPMI 1640 Medium w/25mM HEPES & L-Glutamine, Biowest. 10% heat-inactivated fetal bovine serum (FBS) (PAA Laboratories) and 1% penicillin/streptomycin, Sigma Aldrich, (St Louis, US) were supplemented into the cell cultures and maintained in a humidified incubator at 37°C in atmosphere of 5% CO_2.

MTT Assay

A slightly modified method of Hazalin *et al*. (2009) was used in this MTT assay. HCT116 cells were plated on 96 well plated at a density of 7,000 cells per well and were incubated for 24 hours at 37°C. A serial of dilution (0.01 – 100 μM) for ligand and complexes were prepared before being added to each well. The cells were treated with the compounds and incubated at the temperature of 37°C for 72 hours. 50 mL of aqueous MTT solution of (0.06 mol/L) (Sigma) was then added to each well and plates were incubated at 37°C for another four hours. The MTT solution was decanted off and the formazan crystal was extracted from cells with dimethylsulfoxide (DMSO) (Merck) into each well. The colour was measured with 96-well ELISA plate reader at 450 nm. The dose-response curve was plotted to determine the concentration of compounds required to kill 50% of the cell population (IC_{50}).

Results and Discussion

The synthesis of tetranuclear complexes only needed 10 minutes of microwave irradiation in 10 mL of ethanol:chloroform (7:3 volumetric ratio). There was a significant reduction in reaction time and amount of solvent needed when this method was compared with the conventional reflux method that requires 12-24 hours of reflux in 20 mL of solvent (Bahron *et al.,* 2017). Thus, the electrical power and cooling water consumption were greatly reduced.

Being derived from *meta*-phenylenediamine instead of the more commonly reported *ortho*-penylenediamine, the two azomethine N donor atoms in L are 3-atom apart, i.e., more spread away, making it sterically difficult for both N donors in L to chelate the same metal. As such, two L moieties were bridged by four metal ions during complexation through azomethine N, phenolic O and methoxy O as proposed in Scheme 2. The analytical data and physical properties for the L, $Cu_4(L)_2$, $Co_4(L)_2$ and $Zn_4(L)_2$ are summarized in Table 1. Microanalytical data of C, H, N percentages supported the proposed M:L ratio of 2:1 for the metal complexes. The molar conductivity of all complexes at room temperature were much lower than 40 $\Omega^{-1}cm^2mol^{-1}$ expected for mono-electrolytic species (Laidler & Meiser, 1982) indicating the non-electrolytic nature of the complexes.

Table 1: Physicochemical data for L, $Cu_4(L)_2$, $Co_4(L)_2$ and $Zn_4(L)_2$

Compound	Molecular Formula (RMM)	Colour	Yield (%)	Melting Point (°C)	Elemental Percentages Found (Calculated)			μ_{eff} (B.M.)	Molar Conductivity, Λ_m ($\Omega^{-1}cm^2mol^{-1}$)
					C (%)	H (%)	N (%)		
L	$C_{22}H_{20}N_2O_4$ (376.41)	Orange	95.8	134-136	70.18 (70.12)	5.15 (5.36)	7.14 (7.44)	-	-
$Cu_4(L)_2$	$C_{44}H_{36}Cu_4N_4O_8(CH_3CO_2)(H_2O)_3$ (1116.07)	Brown	31.6	> 300	49.02 (49.50)	4.28 (4.06)	5.34 (5.02)	1.85	7.73
$Co_4(L)_2$	$C_{44}H_{36}Co_4N_4O_8(H_2O)$ (1002.54)	Dark brown	40.8	> 300	52.11 (52.71)	4.89 (3.82)	4.98 (5.59)	3.84	18.28
$Zn_4(L)_2$	$C_{44}H_{36}N_4O_8Zn_4(H_2O)$ (1028.54)	Yellow	33.6	>300	51.80 (51.39)	5.24 (5.72)	4.35 (5.45)	-	0.43

Infrared Spectroscopy

The assignments of significant infrared peaks for all compounds are given in Table 2. The spectra of the complexes (Figure 1) show that the strong absorption peak of the azomethine ν(C=N) at 1617 cm^{-1} in L was shifted 7-13 cm^{-1} to lower frequencies in the metal complexes, as similarly reported by Oladipo *et al.* (2019), indicating the participation of N donor atom in the complexation. The complexation reduced the energy of the C=N, coinciding with the reduction of p-electron density due to the inductive effect of the donation of the lone pair of electrons on N.

The ν(CO) phenolic at 1273 cm^{-1} and ν(C-O) methoxy at 1251 cm^{-1} in L show shifting to lower wavenumbers upon complexation. This observation was also reported by Manna *et al*. (2019). This shifting of frequencies may be attributed to the deprotonation of phenolic O upon complexation and the involvement of methoxy O with the metal centres as a result of complexation to give stable six-membered rings. The appearance of a new weak peak of ν(M-N) and ν(M-O) at range 525-542 and 424-441 cm^{-1} was observed in the spectra of the complexes, indicating the coordination of azomethine N and phenolic O with the metal centers, the trend of which was similarly reported previously (Bahron *et al.,* 2011). The absorption peak of acetate in $Cu_4(L)$ complexes was observed at 1597 cm^{-1}.

Table 2: Significant infrared absorption frequencies in ligand and tetranuclear complexes

Compounds	Frequency (cm^{-1})					
	ν(C=N)	ν(Acetate)	ν(C-O) Phenolic	ν(C-O) Methoxy	ν(M-N)	ν(M-O)
L	1617	-	1273	1251	-	-
$Cu_4(L)$	1605	1597	1245	1226	671	441
$Co_4(L)$	1602	-	1242	1219	651	425
$Zn_4(L)$	1608	-	1242	1200	667	424

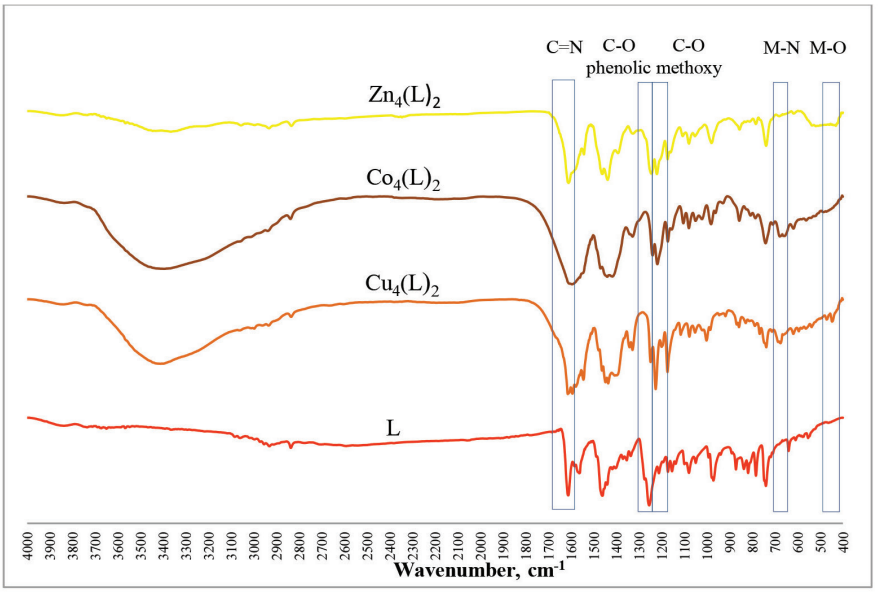

Figure 1: IR spectra for L and its tetranuclear complexes

[1]H and [13]C Nuclear Magnetic Resonance Spectroscopy

The [1]H NMR spectrum and data of L taken in DMSO-*d* are shown in Figure 2 and Table 3, respectively. The [1]H NMR of L was characterized by four of chemical shifts assigned to phenolic, azomethine, phenyl and methoxy protons, in concordance to literature values (Mendu *et al.,* 2015). The [1]H NMR for Zn(II) complexes cannot be obtained due to their insolubility, whereas the copper and cobalt complexes are paramagnetic and not suitable for NMR analysis. The peaks of phenolic, azomethine and methoxy proton appeared at

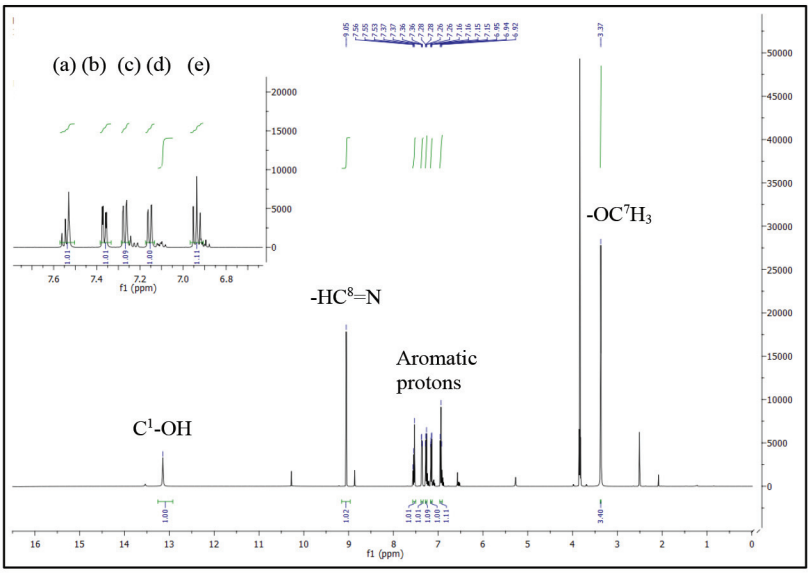

Figure 2: [1]H NMR spectrum of L

Table 3: ^{1}H NMR data of the ligand L

Type of Protons	Chemical Shift, δ (ppm)	J Coupling, Hz	Number of Hydrogen
C^{1}-OH	13.15(s)	NA	1
N=C^{8}H	9.05(s)	NA	1
Aromatic			
C^{10}-H(a)	7.56(m)	NA	1
$C^{11,14}$-H(b)	7.55(m)	NA	1
C^{3}-H(c)	7.39(dd)	^{3}J= 2.0, ^{4}J= 7.9	1
C^{5}-H(d)	7.16(dd)	^{3}J=1.3, ^{4}J=7.9	1
C^{4}-H(e)	6.94(t)	^{4}J=7.9	1
C-O$C^{7}H_{3}$	3.37(s)	NA	3

s=singlet, m=multiplet, dd=doublet of doublet, t=triplet, NA=not applicable

13.15, 9.05 and 3.37 ppm, respectively. The peak of hydroxyl proton appeared downfield at 13.15 ppm as a strong singlet due to the deshielding effect of electronegative O and possible inter- or intramolecular H-bonding. The chemical shift for methoxy protons was found at the upfield region of 3.37 ppm as a sharp singlet peak whereas aromatic protons appeared as multiplets in the range 6.94-7.55 ppm. The values of the J-coupling constant, 1-3 and 6-9 Hz, are supporting evidence for the presence of *ortho* and *meta* hydrogens.

The ^{13}C NMR spectrum (Figure 3) and data (Table 4) of L, recorded sharp peaks representing the non-equivalent carbon atoms in L. The ^{13}C peak for phenolic was observed at 163 ppm, azomethine at 51 ppm, benzene C atoms in the range 149-113 ppm and methoxy at 56 ppm, as similarly observed by other researchers (Iftikhar *et al.,* 2017; Akila *et al.,* 2013; 2012; Reiss *et al.,* 2014).

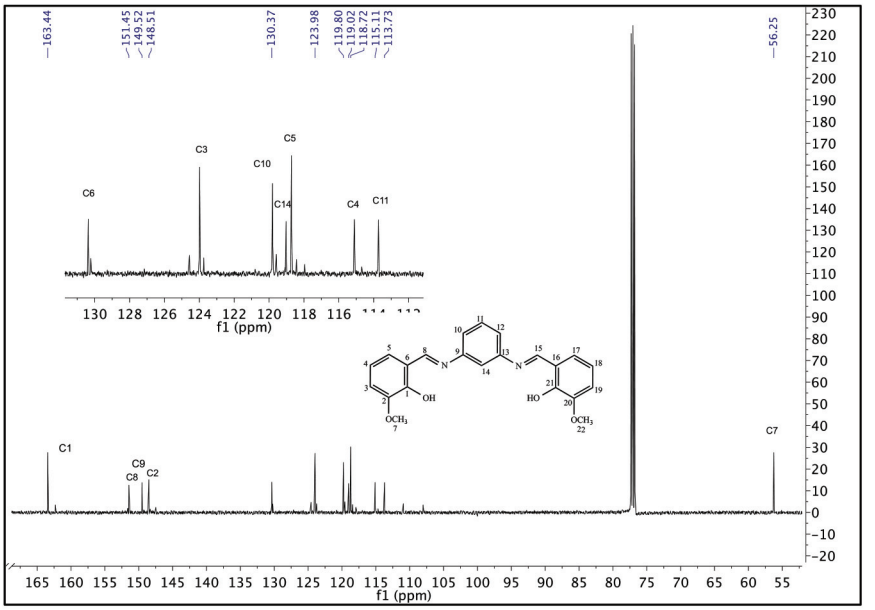

Figure 3: ^{13}C NMR spectrum of L

Table 4: ^{13}C NMR Data for the ligand L

Assignments	Chemical Shift δ (ppm)											
	C1-OH	N=C^{8}-H	C^{9}-H (Ar.)	C-H^{2} (Ar.)	C^{6}-H (Ar.)	C^{3}-H (Ar.)	C^{10}-H (Ar.)	C^{14}-H (Ar.)	C^{5}-H (Ar.)	C^{4}-H (Ar.)	C^{11}-H (Ar.)	OC^{7}H$_3$
L	163.44	151.45	149.52	148.51	130.37	123.98	119.80	119.02	118.72	115.11	113.73	56.25

Notes: Ar = Aromatic

Mass Spectrometer

L ligand was characterized by ESI-MS spectrometry in the positive ion mode. The mass spectrum of the ligand (Figure 4) shows an intense molecular ion peak at m/z = 377, corresponding to the $[C_{22}H_{20}N_2O_4]+H^+$ species which is in good agreement with the proposed structure (calc. RMM of L = 376.41). The molecular ion peak at m/z = 243 corresponds to the remaining fragment of L upon decomposition of one of the $[C_8H_7O_2]$ i.e., the 2-methoxy-6(l^{1}-methyl) phenol moieties, whereas the m/z = 108.9 refers to the remaining fragment after the decomposition of the second $[C_8H_7O_2]$.

UV-Visible Spectroscopy and Magnetic Susceptibility

The electronic spectral data and magnetic moment of the compounds were recorded at room temperature and shown in Table 5. The electronic spectra (Figure 5) show three main bands of L at 232, 277 and 304 nm. The highest energy bands are assigned to π–π* transitions within benzene rings. Moderate energy bands can be assigned to n–π* transitions within C=O and C=N groups (Saif *et al.,* 2016). While all complexes displayed a red shifting of the absorption band of π–π* (C=C benzene), π–π*(C=N), n–π* at range 233-238 nm, 282-294 nm and 320 nm, respectively, due to the donation of a lone pair of electrons to the metal and hence the coordination of azomethine to the metal ions (Bazarganipour & Salavati, 2016). The broad band in the region 397-426 nm observed in the spectra of all complexes was assigned as ligand to metal charge transfer (LMCT).

The effective magnetic moment, μ_{eff}, of $Cu_4(L)_2$ found was 1.85 B.M., close to the theoretical spin only magnetic moment, $\mu_{so,}$ the value of 1 unpaired electron of 1.73 B.M. This is in agreement with Cu(II) d^9configuration. The geometry of Cu(II) cannot depend on this value alone as all geometries would give the same magnetic moment of 1 unpaired electron. The $Co_4(L)_2$ revealed μ_{eff} of 3.84 B.M., indicative of the presence of three unpaired electrons, expected for a tetrahedral Co(II) d^7. The μ_{eff} value ruled out square planar geometry of Co(II) complexes that would show only 1 unpaired electron. This observation is close with previous report by Bakar *et al*. (2011).

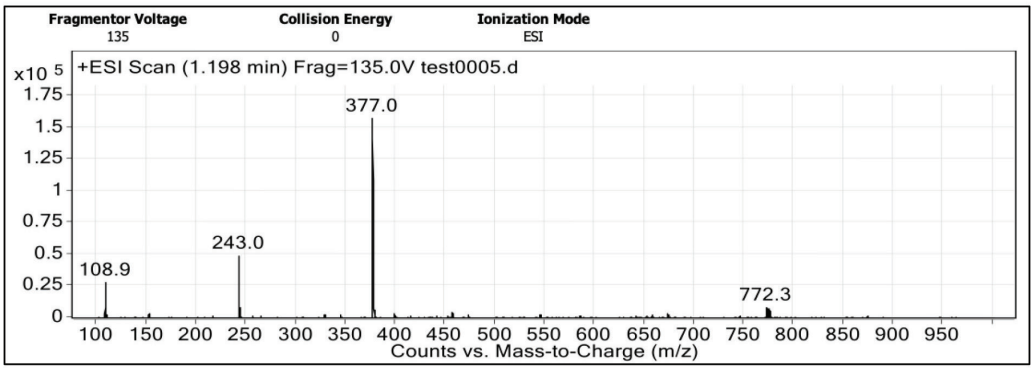

Figure 4: Mass spectrometry spectrum of L

Table 5: Magnetic effective moment, μ_{eff} and electronic spectral data of L, $Cu_4(L)_2$, $Co_4(L)_2$ and $Zn_4(L)_2$

Compounds	μ_{eff}, B.M.	λ_{max}, cm^{-1} (Molar Absorptivity, e)	Transition Assignment
L	-	232 (13301), 277 (9833), 304 (10996)	π–π^*(C=C benzene), π–π^*(C=N), n–π^*
$Cu_4(L)_2$	1.85	233 (14656), 294 (11165), 414 (4689)	π–π^*(C=C benzene), π–π^*(C=N), LMCT
$Co_4(L)_2$	3.84	237 (9968), 282 (7167), 397 (2701)	π–π^*(C=C benzene), π–π^*(C=N), LMCT
$Zn_4(L)_2$	-	238 (4274), 282 (2401), 320 (2619), 426 (923)	π–π^*(C=C benzene), π–π^*(C=N), n–π^*, LMCT

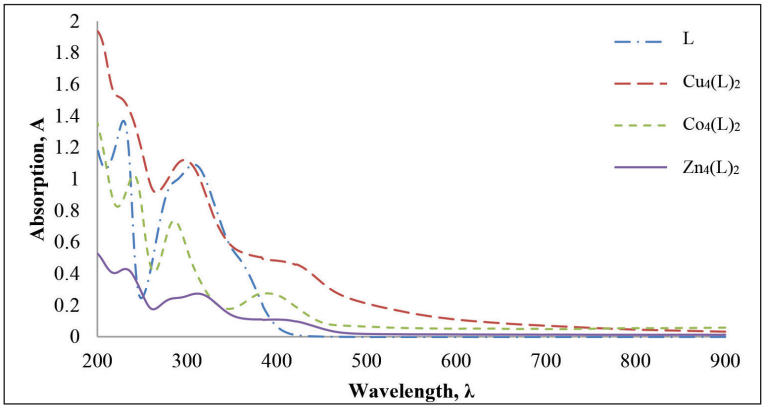

Figure 5: UV-Visible spectra of ligand and complexes

The $Zn_4(L)_2$ complex was diamagnetic as expected of a d^{10} electron configuration. Thus, the stereochemistry cannot be investigated via its magnetic moment and may be determined by consideration of size, electrostatic forces and covalent bonding forces (Kavitha & Lakshmi, 2017) as well as crystallography.

Thermogravimetric Analysis (TGA)

The ligand L and its $Cu_4(L)_2$, $Co_4(L)_2$ and $Zn_4(L)_2$ complexes were subjected to thermogravimetric analysis in the temperature range of 35-450°C to investigate the thermal stability and to determine the presence of water in their lattices. The thermal decomposition data below 300°C for the departure of water molecules is presented in Table 6. The ligand underwent no

Table 6: Thermal decomposition data of L, $Cu_4(L)_2$, $Co_4(L)_2$ and $Zn_4(L)_2$ for the departure of lattice water

Compound	Molecular Formula	Decomposition Temperature for Water (°C)	Weight Loss (%)		Number Water Molecules
			Found	Calculated for Loss of All Water	
L	$C_{22}H_{20}N_2O_4$	Not detected	-	-	0
$Cu_4(L)_2$	$C_{44}H_{36}Cu_4N_4O_8$	36-110	5.8	4.84	3 lattices
$Co_4(L)_2$	$(CH_3CO_2)(H_2O)_3$	100-300	2.2	1.8	1 coordinated
$Zn_4(L)_2$	$C_{44}H_{36}Co_4N_4O_8(H_2O)$	36-175	1.9	1.75	1 lattice

decomposition below 200°C, indicating that no water molecules were present.

All three complexes indicated the presence of water molecules, having partial thermal decomposition occurring at temperatures between 36-300°C for the departure of lattice and coordinated water molecules. Lattice water molecules were expected to depart at lower temperatures below 150°C and coordinated water at higher temperatures above 150°C (Anupama *et al.,* 2016). The complexes $Cu_4(L)_2$ and $Zn_4(L)_2$ revealed that the complexes were not thermally stable as they started to undergo decomposition at quite a low temperature of 36°C. For $Cu_4(L)_2$. The decomposition for equivalence of three lattice water molecules with a mass loss of 5.8% (calcd. 4.84%) was detected at the temperature range 36-110°C. For $Zn_4(L)_2$, a similar analysis revealed that equivalence of 1 lattice water was lost at 36-175°C. The $Co_4(L)_2$ complex underwent decomposition for equivalence of 1 coordinated water molecule at higher temperature of 100-300°C.

Structure Description of Lig and L

The L ligand crystallized in the monoclinic system with the space group of C2/c, a = 19.6783(8) Å, b = 6.8819(2) Å, c = 29.8080(11) Å, a (90°), b (108.62°(4)), g (90°), Z = 8 and V= 3825.4(3) $Å^3$. The crystallographic data and refinement parameters are summarized in Table 7.

The molecular structure of ligand L with the atomic labeling scheme, is presented in Figure 6. The crystal structure is not planar as both terminal benzene ring (C1 - C6) and (C15 - C20) were slightly twisted from the central benzene ring (C8-C13) with torsion angle of 33.18° and 35.14°, respectively. The phenol group and methoxy group at (C1 and C6) and (C16 and C17) bonded at the terminal benzene are coplanar with the attached benzene rings with torsion angle of 2.4(2)° and 0.5(2)°, respectively.

The selected bond length and bond angle are listed in Table 8. The bond length of N(1)-C(8) and N(2)-C(12) are the same with a distance of 1.418(2) Å and 1.419(2) Å, respectively. There are slightly different bond angle C(7)-N(1)-C(8) and C(14)-N(2)-C(12) at 121.27(14)° and 120.78(15)°, respectively, proved that the crystal structure is not in planar. A comparable crystal structure of the analogous $C_{22}H_{22}N_2O_4$, has been reported by Al-douh *et al.* (2007).

In the crystal structure, the molecules are linked by intermolecular hydrogen bond of C3—H3---O1 and C4—H4A---O2 to form crystal packing that is stacked along *b* axis (Figure 7). The molecular conformation is stabilized by two intramolecular hydrogen bonds O2—H2---N1 and O4—H4---N2. The intramolecular and intermolecular hydrogen bonds are listed in Table 9.

Anticancer Screening

Metal complexes can interact with DNA through two general modes of action, which are covalent crosslinking and intercalation (Packianathan *et al.,* 2017; Damercheli *et al.,* 2015). In the current work, the complexes are likely to bind to the DNA through non-covalent intercalation mode, because being planar and containing two or three bonded aromatic rings, the complexes possess the molecular requirements for intercalation (Sundquist & Lippard, 1990). Intercalation interaction involves the insertion of the hetero-aromatic moiety, sliding between two neighbouring base pairs of DNA, to which it is held by weak Van der Waals forces. The intercalating surface is sandwiched tightly between the aromatic heterocylic base pairs and stabilized electronically in the helix by π-π stacking and dipole moment (Long & Barton, 1990). It was also reported that the ligands can interact with DNA via external electrostatic binding between OH moieties of the ligand with phosphate backbone of DNA (Kalarani *et al.,* 2020). Previous studies by Ambika *et al.* (2019) have reported that the Schiff base complexes was interact with DNA via intercalation mode by direct strand scission or base modification that can lengthen and unwind the DNA and induce apoptosis process. However, in this study, the exact cellular anticancer binding mechanisms

Table 7: Crystallographic data and refinement parameters for L ligand

Compound	L
Identification code	L
Empirical formula	$C_{22}H_{22}N_2O_4$
Formula weight	376.41
Temperature (K)	293 (2)
Wavelength (Å)	0.71073
Crystal system	Monoclinic
Space group	C2/c
Unit cell dimensions (Å)	
a = 90°	a = 19.6783(8)(Å)
b = 108.62°(4)	b = 6.8819(2)(Å)
g = 90°	c = 29.8080(11)(Å)
V ($Å^3$)	3825.4(3)
Z	8
$Density_{calc}$ ($Mg\ m^{-3}$)	1.307
Absorption coefficient (mm^{-1})	0.091
F (000)	1584
Crystal dimension (mm)	0.50 x 0.32 x 0.18
Theta range for data collection	3.314 to 29.403°
Index ranges	-24<=h<=27, -9<=k<=9, -40<=l<=40
Independent reflections	4783 [R_{int} = 0.0234]
Completeness to theta = 25.242°	99.5 %
Goodness-of-fit on F^2	1.087
Final R indices	R_1 = 0.0508, wR_2 = 0.1273
R indices (all data)	R_1 = 0.0760, wR_2 = 0.1418

needs to be clarified in future studies to confirm the mode of binding of metal complexes and ligand to the DNA strand.

Figure 8, Figure 9 and Table 10 show dose-response curves, IC_{50} graph and IC_{50} data for the free ligand and complexes. The ligand

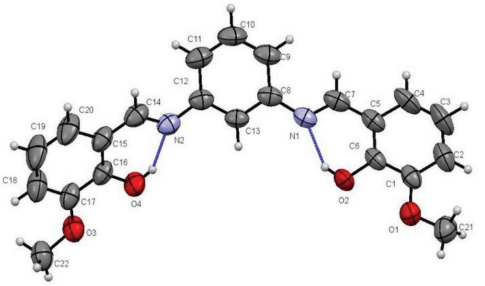

Figure 6: ORTEP diagram of the L ligand drawn at 50% probability ellipsoids

L revealed the IC_{50} value of 60.25 ± 8.30µM revealed that ligand itself has some ability to intercalate with the DNA of HCT116, retarding its growth, hence killing it. It is interesting to note that all complexes exhibited more potent anticancer activity than their parent ligand, L. The copper complex, $Cu_4(L)_2$, was the most potent anticancer with IC_{50} recorded at 6.56 ± 1.26 µM, quite comparable to the standard 5-FU with reported IC_{50} of 4.6 µM (Kumar et al., 2015). The IC_{50} of $Co_4(L)_2$ and $Zn_4(L)_2$ were 34.73 ± 2.64 µM and 20.08 ± 1.32 µM, respectively. The $Co_4(L)_2$ and $Zn_4(L)$ shows a better activity compared to reported by Arafath *et al.* (2017), Parekh *et al.* (2017) and Hassan *et al.* (2017). The relative cytotoxicity of ligand and its complexes against colon cancer cell is in the order of $Cu_4(L)_2$> $Zn_4(L)_2$> $Co_4(L)_2$> L.

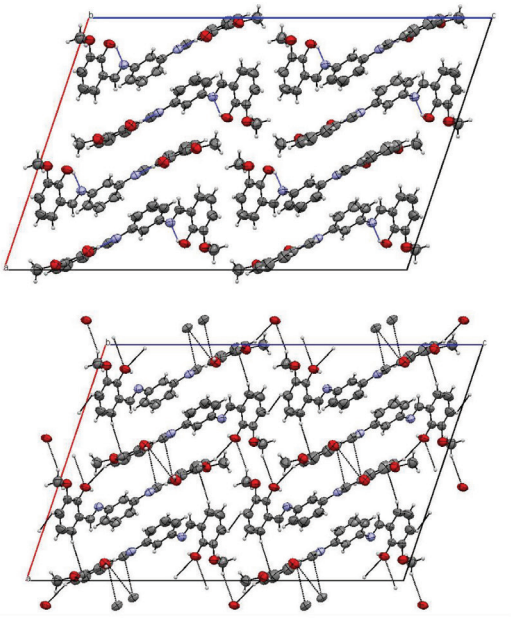

Figure 7: The crystal packing of the L viewed along b axis. The dashed line represents the hydrogen bonds

Copper(II) complexes show the highest exhibition because they can cleave DNA through oxidative and hydrolytic pathways, cell apoptosis via intrinsic reactive oxygen species (ROS) mediated mitochondrial pathway due to excessive production of ROS and hence, are found more active than other complexes (Singh *et al.,* 2020). The redox behaviour of copper(II) is flexible which assists the complexes to form

Table 8: Significant bond length (Å) and angles (°)

Bond Lengths (Å)	
N(1)-C(8)	1.418(2)
N(2)-C(12)	1.419(2)
N(1)-C(7)	1.282(2)
N(2)-C(14)	1.280(2)
Bond Angles (°)	
C(7)-N(1)-C(8)	121.27(14)
C(14)-N(2)-C(12)	120.78(15)
N(1)-C(7)-C(5)	122.41(15)
N(2)-C(14)-C(15)	122.44(16)
N(1)-C(7)-H(7)	118.8
N(2)-C(14)-H(14)	118.8

Table 9: Intramolecular and intermolecular hydrogen bonds (Å, °)

D-H...A	D-H (Å)	H...A (Å)	D-A (Å)	D-H…A (°)
O(2)-H(2)...N(1)	0.82	1.87	2.5972(18)	146.6
O(4)-H(4)...N(2)	0.82	1.87	2.5956(18)	147.1
C(3)-H(3)...N(1)	0.93	2.53	3.3987(1)	155
C(4)-H(4A)...O(2)	0.93	2.49	3.3088(1)	147

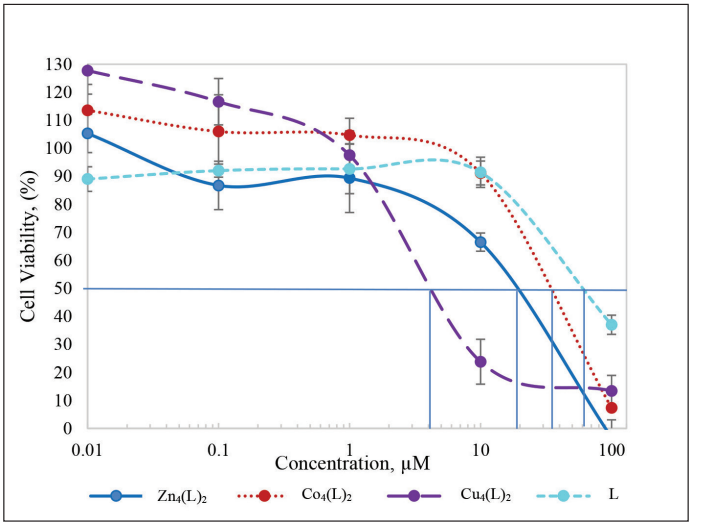

Figure 8: IC_{50} dose-response curves of L, $Cu_4(L)_2$, $Co_4(L)_2$ and $Zn_4(L)_2$

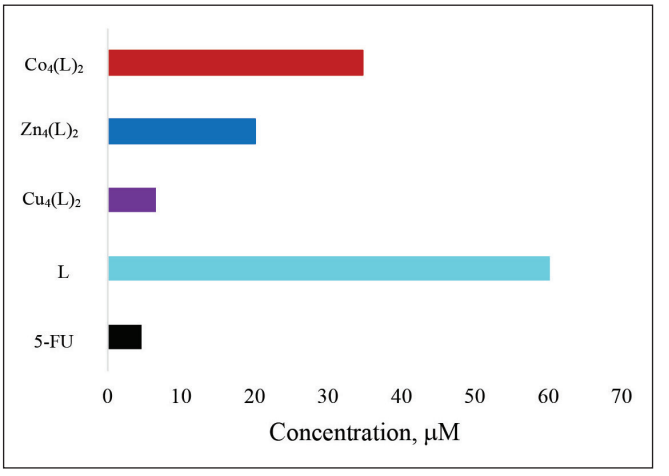

Figure 9: IC_{50} graph of L, $Cu_4(L)_2$, $Co_4(L)_2$ and $Zn_4(L)_2$

Table 10: IC_{50} for L and its tetranuclear metal complexes

Compound	L	$Cu_4(L)_2$	$Zn_4(L)_2$	$Co_4(L)_2$
IC_{50}, µM	60.25 ± 8.30	6.56 ± 1.26	20.08 ± 1.32	34.73 ± 2.64

more potent and clinically effective drugs. However, the properties of copper complexes are mostly determined by the nature of ligands and donor atoms that coordinated to the metal ion (Marzano *et al.,* 2009).

Conclusion

A novel series of tetranuclear metal complexes of Cu(II), Co(II) and Zn(II) were successfully synthesized via microwave irradiation method from a Schiff base ligand derived from phenylenediamine. The structural features were elucidated from their elemental analyses, magnetic susceptibility, molar conductance, TGA, IR, NMR and UV-Visible spectroscopy. Anticancer screening was performed against colon cancer cell line (HCT116). From IC_{50} values, the metal complexes revealed greater anticancer activities compared to free ligand with $Cu_4(L)_2$ showing the highest activity having IC_{50} of 6.56±1.26 μM.

Acknowledgements

The authors wish to thank Universiti Teknologi MARA (UiTM) for the research funding 600-RMC/GPK 5/3 (005/2020) and the Malaysian Ministry of Higher Education for the MyBrainSc scholarship. Universiti Teknologi MARA and Universiti Malaya are gratefully acknowledged for the research facilities provided.

References

Abd El-Wahab, Z. H., & El-Sarrag, M. R. (2004). Derivatives of Phosphate Schiff Base Transition Metal Complexes: Synthesis, studies and biological activity. *Spectrochimica Acta - Part A: Molecular and Biomolecular Spectroscopy*, *60*(1-2), 271-277.

Agilent Technologies. (2014). *CrysAlisPro*. Santa Clara, CA, USA.

Ahamad, M. N., Iman, K., Raza, M. K., Kumar, M., Ansari, A., Ahmad, M., & Shahid, M. (2019). Anticancer properties, apoptosis and catecholase mimic activities of dinuclear cobalt(II) and copper(II) Schiff base complexes. *Journal of Bioorganic Chemistry*, (December 2019).

Akila, E., Usharani, M., Vimala, S., & Rajavel, R. (2012). Synthesis, spectroscopic characterization and biological evaluation studies of mixed ligand Schiff base with metal (II) complexes derived from o-phenylene diamine. *Chem. Sci. Rev. Lett.*, *1*, 181-194.

Akila, E., Usharani, M., Maheswaran, P., & Rajavel, R. (2013). Spectral, magnetic, biocidal screening and DNA cleavage studies of binuclear metal(II) complexes of tetracoordinate Schiff base ligand of 3, 30-dihydroxy benzidine. *Int. J. Rec. Sci. Res.*, *4*, 1497-1503.

Al-douh, M. H., Hamid, S. A., Ng, S., & Fun, H. (2007). Experimental. *Acta Crystallographica Section E Structure Reports Online*, *E63*(2007), 3570-3571.

Al-douh, M. H., Hamid, S. A., Ng, S., & Fun, H. (2007). 6,6'-Dimethoxy-2,2'-[m-phenylene- bis(nitrilomethylidyne)] diphenol. *Acta Crystallographica Section E Structure Reports Online*, *E63*(2007), 3570-3571.

Al-Shaalan, N. H. (2011). Synthesis, characterization and biological activities of Cu(II), Co(II), Mn(II), Fe(II) and UO 2(VI) complexes with a new schiff base Hydrazone: *O*-hydroxyacetophenone-7-chloro-4-quinoline Hydrazone. *Molecules*, *16*(10), 8629-8645.

Ambika, S., Manojkumar, Y., Arunachalam, S., Venuvanalingam, P., & Akbarsha, M. A. (2019). Biomolecular interaction, anti-cancer and anti-angiogenic properties of Cobalt (III) Schiff Base Complexes, (September 2018), 1-14.

Anupama, B., Aruna, A., Lakshmi, P. J., & Swapna, V. (2016). Synthesis, characterization of metal complexes with anthranilic acid based Schiff base: DNA Binding-Cleavage, antimicrobial, antioxidative and BSA binding studies.

International Journal of Inorganic and Bioinorganic Chemistry, *6*(1), 11-22.

Arafath, M. A., Adam, F., Razali, M. R., Ahmed Hassan, L. E., Ahamed, M. B. K., & Majid, A. M. S. A. (2017). Synthesis, characterization and anticancer studies of Ni(II), Pd(II) and Pt(II) complexes with Schiff base derived from N-methylhydrazinecarbothioamide and 2-hydroxy-5-methoxy-3-nitrobenzaldehyde. *Journal of Molecular Structure*, *1130*(Ii), 791-798.

Bader, N. R. (2010). Applications of Schiff 's Bases Chelates in Quantitative Analysis: A review. *Rasayanjournal Chem*, *3*(4), 660-670.

Bahron, H., Kassim, K., Omar, S. R. S., Rashid, S. H., Fun, H. -., & Chantrapromma, S. (2007). (E,E)-N,N″-bis(4-chlorophenyl) ethylenediamine. *Acta Crystallographica Section E: Structure Reports Online, 63*(2), o558-o560.

Bahron, H., Khaidir, S. S., Tajuddin, A. M., & Illah S. A, K. S. (2017). Synthesis and characterisation of Mononuclear and Tetranuclear Zinc (II) Complexes of Schiff Bases Derived from Phenylenediamine. *PERTANIKA Journal of Science and Technology*, 25, 309-316.

Bahron, H., Khaidir, S. S., Mohd Tajuddin, A., & Ramasamy, K. (2019). Synthesis, characterization and anticancer activity of mono- and dinuclear Ni (II) and Co (II) complexes of a Schiff base derived from o -vanillin. *Polyhedron*, *161*, 84-92.

Bahron, H., Mohd Tajuddin, A., Ibrahim, W. N. W., Hemamalini, M., & Fun, H. -. (2011). Bis{2-[(E)-(4-fluoro-benz-yl)imino-meth-yl]-6-meth-oxy-phenolato} palladium(II). *Acta Crystallographica Section E: Structure Reports Online, 67*(6), m759-m760.

Bakar, A. F. A., Bahron, H., Kassim, K., & Mat Zain, M. (2011). Synthesis, characterization and neurotoxic effect of schiff base ligands and their complexes. *The Malaysian Journal of Analytical Sciences, 15*(1), 93-100.

Bazarganipour, M., & Salavati-Niasari, M. (2016). Synthesis, characterization and chemical binding of a Ni(II) Schiff base complex on functionalized MWNTs; Catalytic oxidation of cyclohexene with molecular oxygen. *Chemical Engineering Journal*, *286*(II), 259-265.

Chakraborty, M., Baweja, S., Bhagat, S., & Chundawat, T. (2012). Microwave assisted synthesis of schiff bases: A Green Approach. *International Journal of Chemical Reactor Engineering*, *10*(1).

Chang, E. L., Simmers, C., & Knight, D. A. (2010). Cobalt complexes as antiviral and antibacterial agents. *Pharmaceuticals*, *3*(6), 1711-1728.

Dave, S., & Bansal, N. (2014). Microwave assisted synthesis of schiff bases complexes via eco - Friendly Greener Methodology. *International Journal of Basic and Applied Chemical Sciences*, *4*(1), 58-66.

Dede, B., Ozmen, I., & Karipcin, F. (2009). Synthesis, characterization, catalase functions and DNA cleavage studies of new homo and heteronuclear Schiff base copper(II) complexes. *Polyhedron*, *28*(18), 3967-3974.

Dolomanov, O. V., Bourhis, L. J.,Gildea, R. J., Howard, J. A. K., Puschmann, H. (2009). OLEX2: A complete structure solution, refinement and analysis program. *J. Appl. Cryst., 42*, 339-341.

Ebrahimipour, S. Y., Sheikhshoaie, I., Kautz, A. C., Ameri, M., Pasban-Aliabadi, H., Amiri Rudbari, H., … Janiak, C. (2015). Mono- and dioxido-vanadium(V) complexes of a tridentate ONO Schiff base ligand: Synthesis, spectral characterization, X-ray crystal structure and anticancer activity. *Polyhedron*, *93*, 99-105.

Ghani, A. A., Bahron, H., Harun, M. K., & Kassim, K. (2014). Schiff bases derived from isatin as mild steel corrosion inhibitors in 1 M HCl. *Malaysian Journal of Analytical Sciences*, *18*(3), 507-513.

G. M. Sheldrick. (1997). *SHELXTL V5.1, Software Reference Manual*. Madison, WI, USA: Brukel AXS Inc.

G. M. Sheldrick. (2015). Acta Crystallogr., Sect. C: Struct. Chem., *71*, 3.

Hassan, A. S., Mady, M. F., Awad, H. M., & Hafez, T. S. (2017). Synthesis and antitumor activity of some new pyrazolo[1,5-a] pyrimidines. *Chinese Chemical Letters*, *28*(2), 388-393.

Hazalin, N. a M. N., Ramasamy, K., Lim, S. M., Wahab, I. A., Cole, A. L. J., & Abdul Majeed, A. B. (2009). Cytotoxic and antibacterial activities of endophytic fungi isolated from plants at the National Park, Pahang, Malaysia. *BMC Complementary and Alternative Medicine*, *9*, 46.

Iftikhar, B., Javed, K., Khan, M. S. U., & Akhter, Z. (2017). Synthesis, characterization and biological assay of Salicylaldehyde Schiff Base Cu(II) complexes and their precursors. *Journal of Molecular Structure*, *1155*, 337-348.

Kassim, K., & Hamali, M. A. (2017). Microwave assisted synthesis and characterisation of Trinuclear Zinc(II) Schiff Base Complexes Derived from *m*-phenylenediamine and Salicylaldehyde. *Scientific Research Journal*, *14*(1), 29-40.

Kavitha, N., & Lakshmi, P. V. A. (2017). Synthesis, characterization and thermogravimetric analysis of Co (II), Ni (II), Cu (II) and Zn (II) complexes supported by ONNO tetradentate Schi ff base ligand derived from hydrazino benzoxazine. *Journal of Saudi Chemical Society*, *21*, S457-S466.

Kumar, P., Narasimhan, B., Ramasamy, K., Mani, V., Mishra, R. K., & Majeed, A. B. A. (2015). Synthesis, antimicrobial, anticancer evaluation and QSAR studies of 3/4-bromo benzohydrazide derivatives. *Current Topics in Medicinal Chemistry*, *15*(11), 1050-1064.

Laidler, K. J., & Meiser, J. H. (1982). *Physical Chemistry*. Benjamin/Cummings. p.281- 3 ISBN 0-8053-5682-7.

Long, E. C., & Barton, J. K. (1990). On Demonstrating DNA Intercalation. *Accounts of Chemical Research, 23*(9), 271-273.

Malinkin, S. O., Moroz, Y. S., Penkova, L. V., Bon, V. V., Gumienna-Kontecka, E., Pavlenko, V. A., Fritsky, I. O. (2012). Facile Synthesis of Cu(II) Complexes of Mono- and bicondensed N donor Schiff base 1H-pyrazolate ligands: Crystal structures, spectroscopic and magnetic properties. *Polyhedron*, *37*(1), 77-84.

Mane, P. S., Salunka, S. M., More, B. S., & Chougule A. M. (2011) Synthesis and structural studies of transition metal complexes with Bidentate Schiff base derived from 3-acetyl-6-methyl-(2H)-pyran-2,4(3H)-dione., *Int J. Basic. Appl. Res*., *1*, 24.

Manna, S., Zangrando, E., Puschmann, H., Manna, S. C., Zangrando, E., Puschmann, H., & Manna, S. C. (2019). Tetranuclear Schiff base copper (II) complexes: Syntheses , crystal structure, DNA / protein binding and catecholase-like activity. *Polyhedron*.

Marzano, C., Pellei, M., Tisato, F., & Santini, C. (2009). Copper complexes as anticancer agents. *Anti-Cancer Agents in Medicinal Chemistry*, *9*(2), 185-211.

Mendu, P., Kumari, C. G., & Ragi, R. (2015). Synthesis, characterization, DNA binding, DNA cleavage and antimicrobial studies of Schiff base ligand and its metal complexes. *Journal of Fluorescence*, *25*(2), 369-378.

Mermer, A., Demirbas, N., Uslu, H., Demirbas, A., Ceylan, S., & Sirin, Y. (2019). Synthesis of Novel Schiff Bases using Green Chemistry Techniques; Antimicrobial, antioxidant, antiurease activity screening and molecular docking studies. *Journal of Molecular Structure*, *18*.

Mesbah, M., Douadi, T., Sahli, F., Issaadi, S., Boukazoula, S., & Chafaa, S. (2018). Synthesis, characterization, spectroscopic

studies and antimicrobial activity of three new schiff bases derived from Heterocyclic Moiety. *Journal of Molecular Structure*, *1151*, 41-48.

Mishra, N., Poonia, K., Soni, S. K., & Kumar, D. (2016). Synthesis, characterization and antimicrobial activity of Schiff Base Ce(III) Complexes. *Polyhedron*, 1-9.

Mohanan, K., Kumari, B. S., & Rijulal, G. (2008). Microwave assisted synthesis, spectroscopic, thermal and antifungal studies of some Lanthanide(II1) Complexes with a Heterocyclic Bishydrazone., *Journal of Rare Earth*., *26*, 16-21.

Nithya, P., Rajamanikandan, R., Simpson, J., Ilanchelian, M., & Govindarajan, S. (2018). Solvent assisted synthesis, structural characterization and biological evaluation of Cobalt(II) and Nickel(II) complexes of schiff bases generated from Benzyl Carbazate and Cyclic Ketones. *Polyhedron*.

Oladipo, S. D., Omondi, B., Mocktar, C., Omondi, B., & Mocktar, C. (2019). Synthesis and structural studies of nickel(II)- and copper(II)-N,N'-diarylforma- midine dithiocarbamate complexes as antimicrobial and antioxidant agent. *Polyhedron*.

Packianathan, S., Utthra, P. P., & Raman, N. (2017). Mixed ligand N4O2 type metal(II) complexes as metallointercalators: Preliminary investigation of DNA binding/ cleavage and antimicrobial efficacy. *Inorganic and Nano-Metal Chemistry*, *1556*(February), 1-40.

Parekh, N. M., Mistry, B. M., Pandurangan, M., Shinde, S. K., & Patel, R. V. (2017). Investigation of anticancer potencies of newly generated Schiff base imidazolylphenylheterocyclic-2-ylmethylenethiazole-2-amines. *Chinese Chemical Letters*, *28*(3), 602-606.

Ray, A., Rosair, G. M., Kadam, R., & Mitra, S. (2009). Three new mono-di-trinuclear cobalt complexes of selectively and non-selectively condensed Schiff bases with N2O and N2O2 donor sets: Syntheses, structural variations, EPR and DNA binding studies. *Polyhedron*, *28*(4), 796-806.

Reiss, M. C., Chifiriuc, E., Amzoiu C. I., Spînu. (2014). Transition metal(II) complexes with Cefotaxime-derived Schiff base: Synthesis, characterization and antimicrobial studies, *Bioinorg. Chem. Appl*., 1-17.

Saif, M., El-Shafiy, H. F., Mashaly, M. M., Eid, M. F., Nabeel, A. I., & Fouad, R. (2016). Synthesis, characterization and antioxidant/ cytotoxic activity of new chromone schiff base nano-complexes of Zn(II), Cu(II), Ni(II) and Co(II). *Journal of Molecular Structure*, *1118*, 75-82.

Saikia, L., Baruah, J. M., & Thakur, A. J. (2011). A rapid, convenient, solventless Green Approach for the synthesis of oximes using Grindstone Chemistry. *Med. Chem. Lett*., *12*, 1.

Saini, S., Pal, R., Gupta, A. K., & Beniwal, V. (2014). Microwave-assisted synthesis and antibacterial study of Hydrazone Schiff ' S Ethylidene) Acetohydrazide and its transition metal complexes. *Der Pharma Chemica*, *6*(2), 330-334.

Shabbir, M., Akhter, Z., Ahmad, I., Ahmed, S., McKee, V., Ismail, H., & Mirza, B. (2017). Copper (II) complexes bearing ether based ON donor bidentate Schiff bases: Synthesis, characterization, biological and electrochemical investigations. *Polyhedron*, *124*, 117-124.

Singh, N. K., Kumbhar, A. A., Pokharel, Y. R., & Yadav, P. N. (2020). Anticancer potency of copper(II) complexes of thiosemicarbazones. *Journal of Inorganic Biochemistry*, *210*, 111134.

Sundquist, W. I., & Lippard, S. J. (1990). The coordination chemistry of platinum anticancer drugs and related compounds with DNA. *Coordination Chemistry Reviews*, *100*(C), 293-322.

Tanaka, K., & Toda, F., (2000) Solvent-free Organic Synthesis., *Chem. Rev*., *100*, 1025.